Licentiate Thesis in Civil and Architectural Engineering

Birch plywood in timber connections

Investigation on the rope effect and full-scale trusses

MATTIA DEBERTOLIS

KTH ROYAL INSTITUTE OF TECHNOLOGY

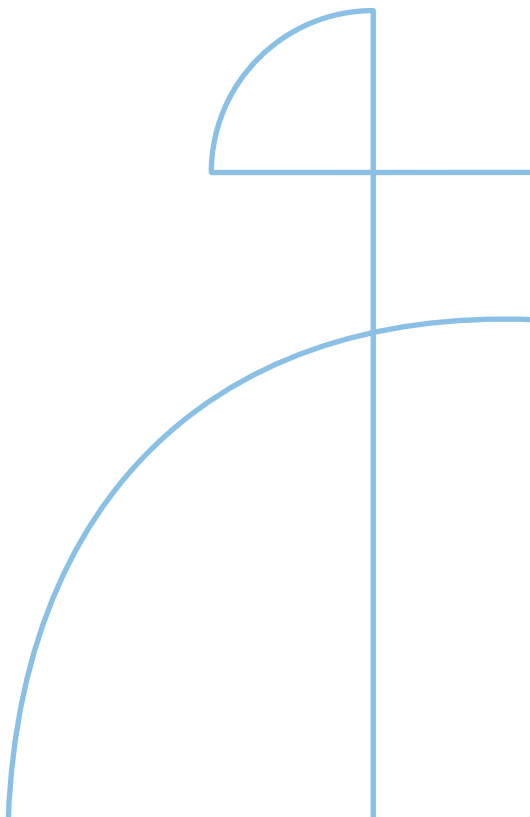

Birch plywood in timber connections

Investigation on the rope effect and full-scale trusses

MATTIA DEBERTOLIS

Academic Dissertation which, with due permission of the KTH Royal Institute of Technology, is submitted for public defence for the Degree of Licentiate of Engineering on Wednesday the 21st of May 2025, at 1:00 p.m. in M108, Brinellvägen 23, Stockholm.

Licentiate Thesis in Civil and Architectural Engineering with Specialization in Building Materials
KTH Royal Institute of Technology
Stockholm, Sweden 2025

TRITA-ABE-DLT-256
ISBN 978-91-8106-269-4

Printed by: Universitetsservice US-AB, Sweden 2025

Abstract

Earlier studies have demonstrated that birch plywood is a viable substitute for steel plates in timber connections, thanks to its excellent mechanical properties, workability, and sustainability. The mechanical properties of birch plywood have been thoroughly investigated concerning key parameters, such as face grain angle and moisture content. Furthermore, its potential use as gusset plates in timber connections has been studied. However, these investigations were mostly limited to uniaxial tension and rather small-scale compared to real applications. Therefore, additional research is needed to further understand the mechanical behaviour of birch plywood, thus ensuring a safe design of such connections. This thesis aims to gain new knowledge on connections with birch plywood plates. The results of this study will then be used to improve the design of such connections, both in terms of safety and structural efficiency.

The influence of the connector type (i.e. smooth dowel or fully threaded screw) was investigated concerning the shear capacity of connections using birch plywood with varying thickness. The results showed that, when utilizing screws, the analytical estimations according to EN1995-1 Eurocode 5 (EC5) significantly underestimate the shear capacity. This is mainly due to EC5's conservative estimation of the so-called "rope effect" contribution to the connection's shear capacity. Moreover, when the number of shear planes was increased from two to four, the discrepancy between EC5's estimation and experimental results substantially increased regardless of the type of fastener. This substantial discrepancy was associated with the failure mode in the inner shear planes.

Furthermore, both glued and mechanical connections were investigated by performing tests on full-scale glulam trusses joined through birch plywood gusset plates. Failure was designed to occur in the plywood plates subjected to a complex stress state. In this investigation, the thickness of these plywood plates was varied between 9, 12 and 21 mm, testing only one specimen for each configuration. The experimental results showed that glued trusses possessed higher load-carrying capacity and almost twice the stiffness of those with mechanical fasteners. Failure occurred in the plywood plates for all trusses with mechanical fasteners and the glued truss with thinner plywood plates (9 mm).

However, the trusses with thicker plates (i.e. 12 and 21 mm) showed glue line failure between the plywood plate and the glulam beam. The analytical estimations for specimens that failed in the plywood plate generally showed good agreement with the experimental capacity, although they exhibited a slight overestimation. This was expected and was attributed to the size effect, as the input strength values of plywood adopted in the analytical estimations were obtained from small-scale tests.

Furthermore, based on the size of the glued area compared to previous studies, bonding strength values were estimated and used in the analytical calculations of the bonding capacity for glued connections. However, these strength values should be further investigated to calibrate the analytical model and obtain more realistic estimations.

In addition, two-dimensional numerical models demonstrated good agreement in predicting the global stiffness of the tested trusses.

For future work, it is suggested to investigate the size effect on the mechanical properties of birch plywood and bonding strength, respectively, to further calibrate and validate the analytical models. Furthermore, more advanced numerical simulations of the truss specimens are suggested.

Keywords
Timber-to-timber connections, birch plywood gusset plates, rope effect, mechanical connections, glued connections

Sammanfattning

Tidigare studier har visat att björkplywood är ett effektivt alternativ till stålplåtar i träförband, främst tack vare dess goda mekaniska egenskaper, bearbetbarhet och hållbarhet. Dessa egenskaper har studerats ingående med avseende på viktiga parametrar såsom fiberriktning och fuktkvot. Dess användning som laskar i träkonstruktioner har även undersökts. Dock har tidigare studier främst varit begränsade till enaxliga dragprov och mindre provkroppar, vilket innebär att ytterligare forskning krävs för att förstå björkplywoodens mekaniska beteende i mer realistiska och komplexa tillämpningar. Syftet med denna avhandling är därför att bidra med ny kunskap om förband med laskar av björkplywood. Resultaten syftar till att förbättra dimensioneringen av sådana förband, med avseende på både säkerhet och strukturell effektivitet.

Typen av fästdon (släta dymlingar eller skruvar) har undersökts i relation till skjuvhållfastheten i förband med varierande plywoodtjocklek. Resultaten visade att EN1995-1 Eurokod 5 (EC5) underskattar skjuvhållfastheten vid användning av skruvar, vilket främst beror på en konservativ uppskattning av den icke-linjära ökningen av motståndet vid glidning som bidrar positivt till förbandets bärförmåga. Vidare ökade avvikelsen mellan de analytiska beräkningarna och de experimentella resultaten avsevärt när antalet skjuvplan ökades från två till fyra, oberoende av typ av fästdon. Denna betydande avvikelse förknippades med brottmoden i de inre skjuvplanen.

Vidare har både limmade och mekaniska förband undersökts genom fullskaleförsök på limträfackverk sammanfogade med skivor av björkplywood. Brott var avsett att initieras i plywooden, vilka utsattes för komplexa spänningstillstånd. Plywoodskivornas tjocklek varierades mellan 9, 12 och 21 mm, och en provkropp testades för varje konfiguration. De experimentella resultaten visade att de limmade fackverken uppvisade högre bärförmåga och nästan dubbelt så hög styvhet som de med mekaniska förband. Vid samtliga fackverk med mekaniska förband, samt det limmade fackverket med de tunnaste plywoodskivorna (9 mm), uppstod brott i plywooden. För de limmade fackverken med tjockare plywood (12 och 21 mm) inträffade dock brott i limfogen mellan plywooden och limträelementet. De analytiska beräkningarna för de prov där brotten uppstod i plywooden överensstämde generellt väl med

de experimentella resultaten, även om en viss överskattning noterades. Detta var förväntat och tillskrivs skalningseffekter, då materialegenskaperna som använts i beräkningarna härrör från småskaliga tester.

Baserat på jämförelser med tidigare studier uppskattades även limhållfasthetsvärden för att inkluderas i de analytiska beräkningarna av bärförmågan i limmade förband. Dessa värden bör dock undersökas vidare för att kalibrera och förbättra de analytiska modellerna.

Därtill visade tvådimensionella numeriska modeller god överensstämmelse med den globala styvheten uppmätt i försöken.

För framtida arbete föreslås en fördjupad undersökning av skalningseffekter på björkplywoodens mekaniska egenskaper samt limhållfasthet, i syfte att vidare kalibrera och validera de analytiska modellerna. Även mer avancerade numeriska simuleringar föreslås.

Nyckelord
Trä-mot-trä-förband, laskar av björkplywood, mekaniska förband, limmade förband

Preface

The work presented in this licentiate thesis was carried out at the Division of Building Materials, Department of Civil and Architectural Engineering, KTH Royal Institute of Technology in Stockholm, Sweden, and at CNR IBE laboratory in San Michele all'Adige, Italy. The author gratefully acknowledges the financial support of the Lars Erik Lundberg Scholarship Foundation. The work has also been supported by the Kamprad Family Foundation (reference number: 20200013) and from Produktion2030, a strategic innovation program supported by Vinnova [reference number: 2021-03681], Swedish Energy Agency, Formas including the industry partners.

Firstly, I would like to express my gratitude to my supervisors Prof. Roberto Crocetti and Prof. Magnus Wålinder for supervising me since my master thesis in 2022, for their valuable guidance, advice and encouragement.

Secondly, I would express my sincere gratitude to Dr. Lars Blomqvist for his valuable technical suggestions and for arranging part of the financial support.

Special thanks to my colleagues and co-authors Dr. Yue Wang and Dr. Tianxiang Wang. This work would not have been possible without your contribution, as well as the thoughts and discussions we shared.

Koskisen, Rothoblaas and Rubner Holzbau are acknowledged for the supply of birch plywood, mechanical connectors, and glulam, respectively. Furthermore, the Swedish Wood Protection Institute (Svenska Träskyddsföreningen) and TMF (Trä- och Möbelföretagen) are also acknowledged for supplying wood materials. Viktor Brolund, Simone Rossi, Andrea Polastri, Diego Magnago and Pietro Rigo are sincerely thanked for their technical support in the preparation and execution of the laboratory tests.

Lastly, but equally important, I would like to thank my family and friends, and most importantly, my girlfriend Jessica Lucchetta, for their endless support.

List of appended papers

This thesis is based upon the following scientific articles referred to in the text by their roman numbers:

Paper I

M. Debertolis, Y. Wang, T. Wang, R. Crocetti, M. Wålinder, Rope effect in mechanical panel-timber connections: A comparison between screws and dowels. Engineering Structures, Volume 332, 2025, 120036, ISSN 0141-0296, https://doi.org/10.1016/j.engstruct.2025.120036.

Paper II

M. Debertolis, Y. Wang, T. Wang, R. Crocetti, M. Wålinder, P. Rigo, A. Polastri, Analytical, experimental and numerical investigation on full-scale glulam trusses joined through birch plywood plates. *Submitted manuscript.*

In the appended papers, the first author planned and performed the majority of the experiments, set up the analytical and numerical models, and wrote the manuscript with the help of the co-authors.

List of abbreviations

EC5	EN1995-1 Eurocode 5
EWPs	Engineered Wood Products
LVDTs	Linear Variable Displacement Transducers
MC	Moisture Content
MUF	Melamine-urea-formaldehyde
WFP	Wood Failure Percentage

Contents

1 Introduction

1.1 Birch plywood in timber connections

Birch is a widely distributed wood species across the Eurasian continent, particularly in northern Europe. Engineered wood products (EWPs), such as plywood, can overcome the limitation of timber's natural shape, improve dimensional stability and reduce its natural variability by redistributing natural defects [1]. Plywood is one of the earliest EWPs to be manufactured and is composed of an uneven number of veneers, which usually have a thickness of a few millimetres. Each veneer is laid up and glued together with the grain direction one perpendicular to the other [2]. Thanks to its cross-layup configuration, plywood is self-reinforced against cracking along the grain and shows significantly lower anisotropic behaviour compared to solid wood. The higher density and superior mechanical performance of birch over softwood species, combined with the cross-laminated configuration of plywood, make birch plywood a promising material for structural applications. Previously, birch plywood has been used, for example in concrete formwork, sub-flooring, decking, or even in aircrafts [3]. Recent research has thoroughly investigated its mechanical properties [4-5] (Figures 1a and b) and shown its potential in timber connections [6-9], for example in timber frame corner joints [10] (Figure 1c), or in moment resisting connections [11] (Figure 1d). Another potential application of birch plywood is in a typical truss node, as shown in Figure 2.

In timber structures, the joints between different members are particularly important, as they are usually the weakest part of the structure [12]. Moreover, they significantly influence the overall behaviour of the structure, including its strength, stiffness, final cost, and most of the design effort [13]. Currently, one of the most common methods used in connections for long-span timber structures involves slotted-in steel plates and mechanical connectors. However, steel has limited workability and requires a very high level of precision during assembly. Furthermore, compared to steel, birch plywood has a lower environmental footprint, is relatively cheap and has a good fire resistance [14]. A comparison between a connection using birch plywood plates and one with slotted-in steel plates and smooth dowels showed that both connection types can achieve similar strengths when considering the number of fasteners that can be

inserted within a specific connection area, which depends on the fastener diameter [15].

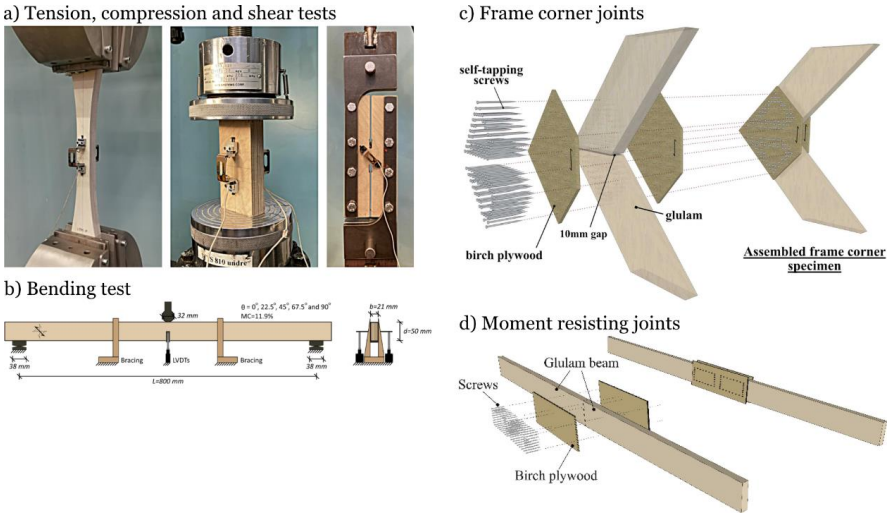

Figure 1: Previous investigations on: a) and b): birch plywood mechanical properties, c) frame corner joints, and d) moments resisting joints with birch plywood plates.

Some studies have shown that EN1995-1 Eurocode 5 (EC5) [16] design model tends to underestimate the actual shear capacity of timber-to-timber connections [15, 17-19]. The design model adopted in EC5 [16] to estimate the lateral load-carrying capacity (also referred to as "shear capacity") and design connections with metal fasteners is based on the Johansen yield theory. In failure modes where the fastener undergoes yielding, the formulas for calculating shear capacity consist of two parts. The first part is the so-called Johansen's theoretical contribution, derived from equilibrium equations, while the second part is the so-called rope effect. The rope effect is activated once a fastener has significantly bent. If this is the case, tensile forces are activated in the fastener, given that it possesses a certain withdrawal capacity. The rope effect enhances a connection's load-carrying capacity and is primarily influenced by factors such as the fastener's surface texture (smooth or threaded) or the presence of washers and nuts at the ends of the fasteners. In the case of connections with screws, the rope effect results from the axial force in the screw, which gives rise to two contributions: a) a force component parallel to the loading direction and b) friction caused by the force component perpendicular to the loading direction. However, according to EC5's formulas [16], the rope effect contribution is limited to a maximum of one-fourth of the fastener's withdrawal capacity or a certain percentage of Johansen's part, whichever is

smaller. Furthermore, EC5 does not give specific guidelines when designing a connection with more than two shear planes.

Furthermore, in previous investigations on birch plywood in connections of timber structures [7-11, 15, 17], the specimen sizes were relatively small compared to real-world applications, and the plywood plates were subjected to simple stress states, such as uniaxial tension. However, in reality, a gusset plate in a truss node, as shown in Figure 2, might be subjected to a very complex state of stresses, including both axial, bending and shear stresses.

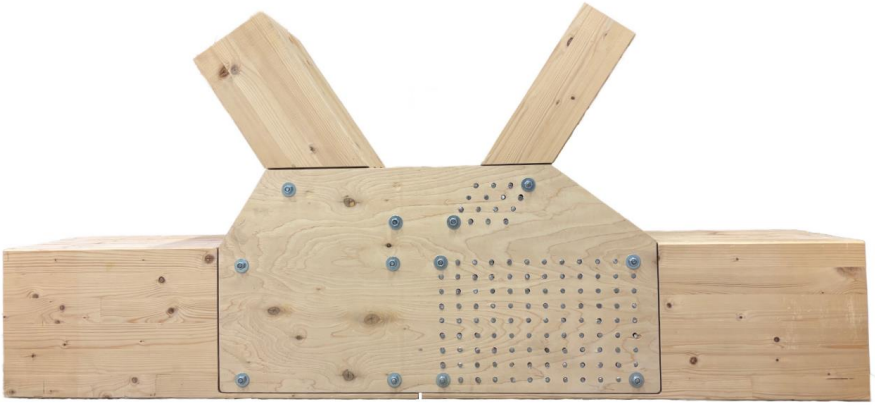

Figure 2: Truss node with plywood gusset plates.

1.2 Aim and objectives

The aim of this thesis is to gain new knowledge on connections with birch plywood plates to improve structural efficiency and ensure a safe design of such connections. Specifically, Paper I aims to investigate the impact of the rope effect and its contribution to the lateral load-carrying capacity of a connection. This was done by testing connections with birch plywood gusset plates in double shear with varying plywood plates' thickness and the type of fastener, i.e. smooth dowels and fully threaded screws. In addition, connections with four shear planes were tested to determine whether the number of shear planes affected the load-carrying capacity and failure mode.

Paper II aims to investigate the overall behaviour of full-scale glulam trusses using birch plywood gusset plates, comparing two types of connections: mechanical and adhesively bonded. The failure was designed to occur in the plywood plate, which was subjected to a complex stress state due to the convergence of three glulam elements at the node. Furthermore, the thickness

of these plywood plates was varied between 9, 12 and 21 mm to investigate different failure modes.

1.3 Thesis structure

This thesis begins with an introductory section outlining the background, motivation, aim, and objectives. Section 2 describes the materials and methods used in the investigations. Section 3 presents and discusses the experimental and analytically predicted results. Lastly, Section 4 summarizes the key findings and proposes future research.

2 Materials and methods

2.1 Birch plywood

The birch plywood panels used in this study are ordinary products produced by Koskisen Oy (Järvelä, Finland). Each panel has a mean density of approximately 680 kg/m^3 [20] and consists of an odd number of veneers, which are laid up with the grain direction perpendicular to the other and adhesively bonded together with phenol formaldehyde resin. The inner veneers have an equal thickness of 1.4–1.5 mm, while the outer face veneers are thinner due to sanding during production. Plywood panels with a nominal thickness of 15, 21, 30 and 42 mm were used in the first paper, while 9, 12 and 21 mm thick panels were used in the second paper. The standard size of plywood panels is 1.2 x 2.4 meters [20], with the face grain parallel to the shorter edge.

Figure 3: Birch plywood panels with varying thicknesses.

2.2 Lateral load-carrying capacity

2.2.1 Experiments

The influence of a) birch plywood plate thickness, which varied between 15 and 42 mm, and b) connector type — either a smooth dowel or a full-threaded screw — on the lateral load-carrying capacity was investigated in connections

with two shear planes. Each of these specimens, which are also referred to as specimens in double shear, consisted of an inner 90 mm thick member of Scots pine structural timber of grade C24 and two outer plywood plates connected via two mechanical fasteners for each connection, as depicted in Figure 4a. Furthermore, specimens with four shear planes, as shown in Figure 4b, which combined two specimens in double shear, were tested to investigate the influence of shear plane numbers on the lateral load-carrying capacity. In this case, the chosen thickness of the plywood plates was consistently 21 mm.

Although EC5 [16] requires pre-drilling for hardwood species, all the specimens with screws were assembled without any pre-drilling. This was done with practical applications in mind, as avoiding pre-drilling allows for faster assembly. Nevertheless, one configuration in double shear with screws and 30 mm thick plywood was assembled after pre-drilling through the entire cross-section 6 mm holes to assess any influence on the load-carrying capacity. For specimens with dowels, 8.5 mm holes were drilled before assembling the connections with dowels with a diameter of 8 mm.

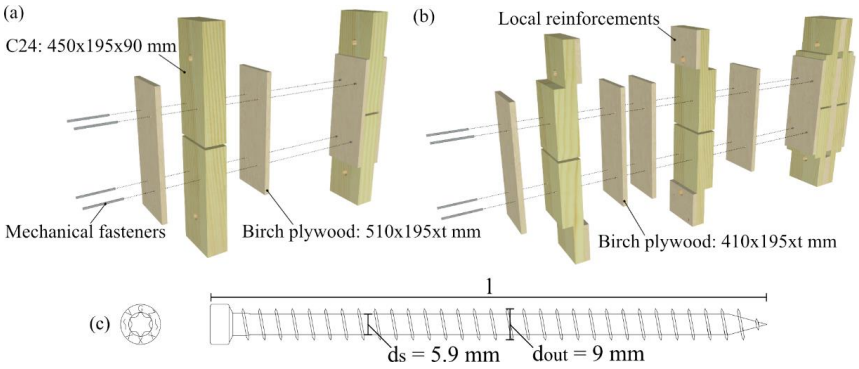

Figure 4: Illustration of specimens' properties: a) two shear planes and b) four shear planes. C) Illustration of Rothoblaas VGZ screw details.

Three replicates were tested for each test series in order to achieve reasonable statistical relevance. As a result, a total of 33 timber-to-timber connection specimens were tested under uniaxial tension, with 27 of them being specimens with two shear planes and 6 of them being specimens with four shear planes.

Fully threaded VGS screws were employed for the specimens in double shear, while fully threaded VGZ screws were used for the specimens with four shear planes. Both types of screws are manufactured by Rothoblaas and have similar mechanical properties, differing only in head shape [21]. The screws had an

outer diameter (d_{out}) of 9 mm and a shank diameter (d_s) of 5.9 mm, as depicted in Figure 4c, while the smooth dowels had a diameter (d_d) of 8 mm.

Four linear variable displacement transducers (LVDTs) recorded the slip between the plywood plates and the structural timber, as shown in Figure 5. The lateral load-carrying capacity of a connection, as defined by ISO 6891-1983 (E) [22], is the highest recorded load within 0 and 15 mm of slip. More details regarding the test setup and procedure are presented in Paper I [23].

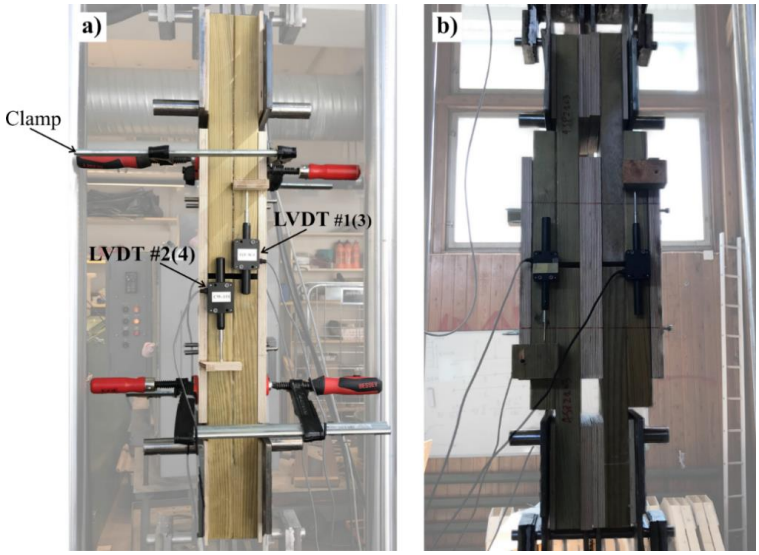

Figure 5: Specimens mounted on the testing machine: a) doweled specimen in double shear, and b) screwed specimen with four shear planes.

All specimens were stored indoors at a temperature of 20°C and approximately 50 % relative humidity for about one month before testing. The measured average moisture content (MC), determined using the oven-dry method in EN 322:1993 [24], and the average density of birch plywood were 6.8 % and 684 kg/m^3, respectively. For the C24 structural timber, these values were 8.9 % and 558 kg/m^3, respectively.

2.2.2 Analytical estimations

The specimens in this study were designed to achieve ductile failure modes with the bending of the fasteners (*mode j* and *k* in Figure 6), which are preferable in structures compared to brittle failure modes. According to EC5 [16], the lateral load-carrying capacity of such failures consists of two contributions: Johansen's theoretical contribution (dowel-effect part) and rope effect contribution.

Johansen's theoretical contribution was derived from equilibrium equations according to Johansen's theory [25], while the rope effect contribution was estimated according to EC5 [16].

For specimens with four shear planes, failure *mode j* was considered unlikely to occur in the inner birch plywood plates due to the symmetry of the connection, whereas failure *mode k* was expected to occur in the inner plates.

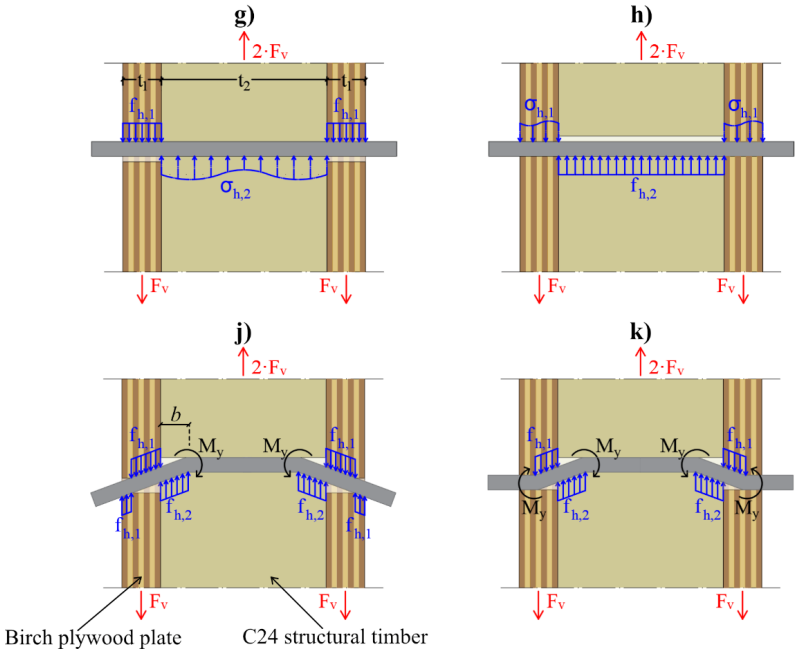

Figure 6: Possible failure modes in panel-to-timber joints with two shear planes.

The formulas used for calculating the lateral load-carrying capacity for each specimen are the following:

$$F_{v,R} = min \begin{cases} f_{h,1} \cdot t_1 \cdot d & \text{Mode } g \quad (1) \\ 0.5 f_{h,2} \cdot t_2 \cdot d & \text{Mode } h \quad (2) \\ \dfrac{f_{h,1} \cdot t_1 \cdot d}{(2+\beta)} \left[\sqrt{2\beta(1+\beta) + \dfrac{4\beta(2+\beta) M_{y,R}}{f_{h,1} \cdot d \cdot {t_1}^2}} - \beta \right] + \dfrac{F_{ax,R}}{4} & \text{Mode } j \quad (3) \\ \sqrt{\dfrac{2\beta}{(1+\beta)}} \sqrt{2 M_{y,R} \cdot f_{h,1} \cdot d} + \dfrac{F_{ax,R}}{4} & \text{Mode } k \quad (4) \end{cases}$$

with

$$\beta = \frac{f_{h,2}}{f_{h,1}} \tag{5}$$

where $F_{v,R}$ is the lateral load-carrying capacity per shear plane per fastener; t_1 and t_2 are the thicknesses of plywood and structural timber, respectively; $f_{h,1}$ and $f_{h,2}$ are the embedment strength of birch plywood and structural timber; d is the fastener diameter; $M_{y,R}$ is the fastener yield moment; β is the ratio between the embedment strengths of the timber elements; and $F_{ax,R}$ is the axial withdrawal capacity of the fastener which contributes to the so-called rope effect. In the case of screws, the effective diameter of the screw (d_{eff}) was used in the calculations which corresponds to 1.1 times the shank diameter and is equal to 6.5 mm [16].

The axial withdrawal capacity of a screw $F_{ax,R}$ was calculated according to EC5 [16] as:

$$F_{ax,R} = \frac{f_{ax} \cdot d \cdot l_{ef} \cdot k_d}{1.2 \cdot cos\alpha^2 + sin\alpha^2} \tag{6}$$

$$f_{ax} = 0.52 \cdot d^{-0.5} \cdot l_{ef}^{-0.1} \cdot \rho^{0.8} \tag{7}$$

$$k_d = min\begin{cases} d/8 \\ 1 \end{cases} \tag{8}$$

where f_{ax} is the withdrawal strength perpendicular to the grain; d is the outer diameter of the screw (d_{out}); l_{ef} is the penetration length of the threaded part; ρ is the wood density; α is the angle between the screw axis and the grain direction; and k_d is a reduction factor that is dependent on the diameter of the fastener.

2.3 Full-scale glulam trusses with birch plywood gusset plates

2.3.1 Experiments

A total of 6 glulam trusses joined at the nodes through birch plywood gusset plates were constructed and tested. Three trusses were joined through Melamine-urea-formaldehyde-based (MUF) glue, while the remaining three through smooth steel dowels with a diameter of 8 mm and a steel grade of C45. As depicted in Figure 7, each truss had a total length of 7.58 m and a height of 1.366 m. The thickness of the central plywood plates varied between 9, 12 and 21 mm, while the thickness of the other plywood plates was consistently 21 mm. The trusses were designed to fail in the central plywood plate, which was

subjected to a complex stress state, avoiding any plastic yielding of the fasteners before failure. Each specimen was labelled according to the connection type (GLU for glued and DOW for doweled) and the thickness of the central plywood plate in millimetres (09, 12 or 21). Further details regarding the design and geometry of the specimens are presented in Paper II [26].

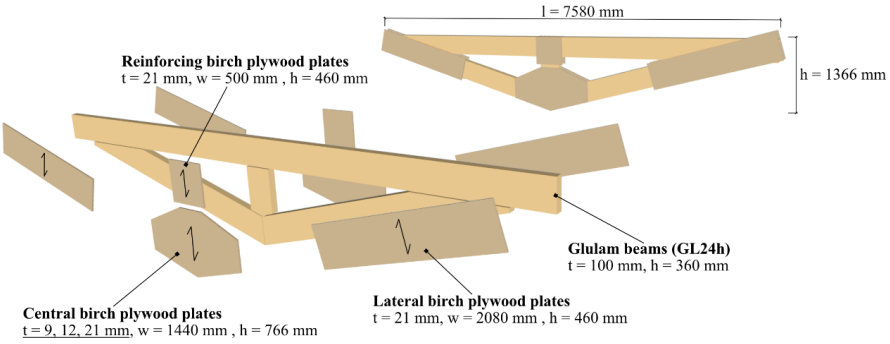

Figure 7: Illustration of the truss specimen geometry.

A gap of 10 mm between each glulam member was kept to have an unambiguous load path through the plywood plates, except between the horizontal glulam member and the vertical post. Furthermore, rectangular plywood plates were glued on the horizontal glulam member, both to reinforce against compression perpendicular to the grain and to restrain possible out-of-plane movements of the vertical post.

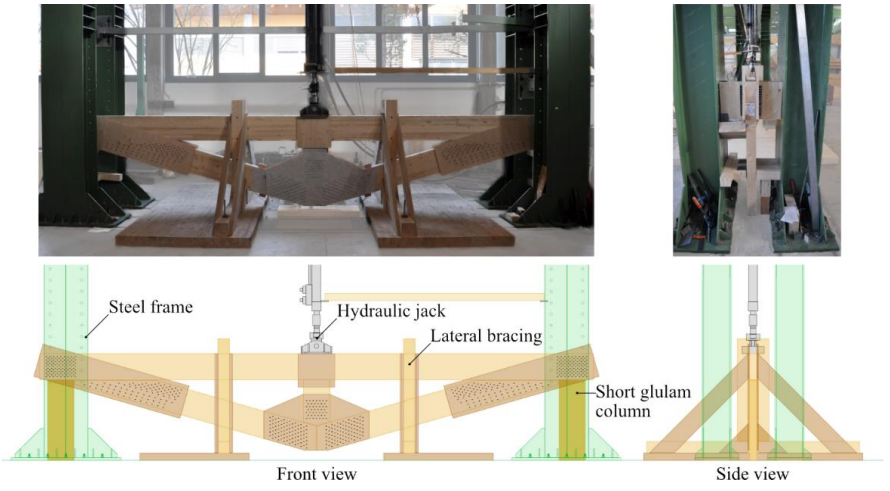

Figure 8: Test setup.

Each truss had a span of 7 m and was supported by two short glulam columns with a height of 1.1 m, as shown in Figure 8. The load was applied on top of the horizontal glulam member with a constant displacement rate of 6 mm/min. In addition, each truss was laterally braced to restrain out-of-plane movements. Furthermore, LVDTs were employed to record absolute and relative displacements around the central plywood plate connection.

The measured average MC, according to the procedure reported in EN 13183 [27], and the average density of birch plywood were 11.1 % and 722.8 kg/m^3, respectively. For the glulam, these values were 15.5 % and 524.2 kg/m^3, respectively.

2.3.2 Prediction models

Analytical models were used to estimate the ultimate load and failure mode for each configuration, while two-dimensional numerical models were developed to predict the global stiffness.

2.3.2.1 Analytical models

Connections with mechanical fasteners were assumed to behave as hinged, while adhesively bonded connections were considered rigid. For trusses with mechanical fasteners, the load was assumed to be applied to the vertical post, which was not connected to the horizontal glulam member. This assumption was made to simplify the calculations, as the vertical load carried by the horizontal glulam beam was not significant. Consequently, in the analytical calculations of the trusses with mechanical fasteners, glulam beams were subjected only to axial forces, as shown in Figure 9a. For all specimens, the tensile force in the central plywood plate was assumed to act within the height given by the spreading angle effect ($h_{bp\_sa\_DOW}$ and $h_{bp\_sa\_GLU}$ in Figure 9), which was previously investigated for birch plywood in [9, 28]. In this study, the spreading angle for mechanical connections was 23°, while for glued connections it was 13°, with a load-to-face grain angle between the inclined glulam beam and the plywood face grain of 74°.

The axial force in the glulam beam (N_{GL_inc}) was converted into components parallel and perpendicular to the central plywood plate's face grain (N_{BP} and V_{BP}). The verification of the plywood plate was done through the following interaction formula that takes into account the combined actions of tension and shear:

$$\frac{N}{R_N} + \frac{V}{R_V} = 1 \tag{9}$$

where

$$R_N = f_{t\_bp\_90} * n * t_{bp} * \left(h_{bp\_sa\_DOW} - 9 * d\right) \tag{10}$$

$$R_V = f_{v\_bp\_0} * n * t_{bp} * \left(h_{bp} - 11 * d\right) \tag{11}$$

where N and V are respectively the normal force and shear force in the plywood plate (N_{BP} and V_{BP} in Figure 9a); $f_{t\_bp\_90}$ and $f_{v\_bp\_0}$ are the tensile and shear birch plywood strengths with 90° and 0° load-face grain angle [4], respectively; t_{bp} is the plywood thickness; d is the fastener diameter; $(h_{bp\_sa\_DOW} - 9 * d)$ and $(h_{bp} - 11 * d)$ are the effective depths of the plywood plate for tension and shear, respectively; and n is the number of shear planes. The effective depths were calculated by subtracting the total area of the fastener holes (number of holes multiplied by the fastener diameter) along the respective measured lengths ($h_{bp\_sa\_DOW}$ or h_{bp}).

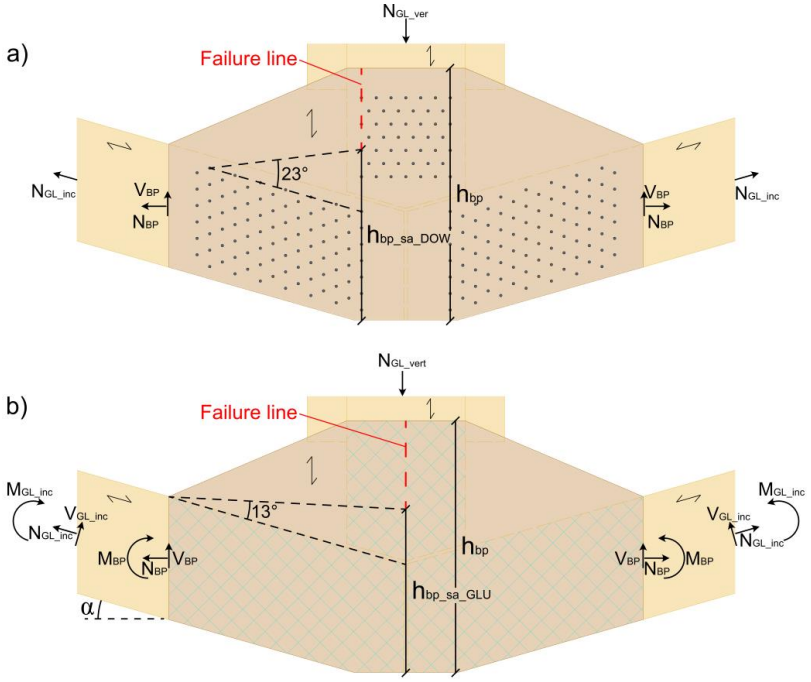

Figure 9: Illustration of spreading angle and internal actions in the central plywood plates for: a) trusses with mechanical fasteners, b) glued trusses.

For glued trusses, the load capacity of the central plywood plate was estimated using the following formula which considers the interaction between normal force, shear force and bending moment [29]:

$$\frac{N}{R_N} + \left(\frac{M}{R_M}\right)^2 + \frac{V}{R_V} = 1 \tag{12}$$

where

$$R_N = f_{t\_bp\_90} * n * t_{bp} * h_{bp\_sa\_GLU} \tag{13}$$

$$R_V = f_{v\_bp\_0} * n * t_{bp} * h_{bp} \tag{14}$$

$$R_M = f_{m\_bp\_90} * \frac{n * t_{bp} * (h_{bp} * \cos(\alpha))^2}{6} \tag{15}$$

where M is the bending moment in the plywood plate (M_{BP} in Figure 9b); $f_{m\_bp\_90}$ is the birch plywood's in-plane bending strength with 90° load-face grain angle [5]; $h_{bp\_sa\_GLU}$ is the spreading angle height for glued trusses; h_{bp} is the height of the plywood plate at midspan; and α is the angle between the glulam beam and the horizontal direction (Figure 9b).

The estimation of the glue line resistance was performed according to the following formula, which considers the contributions of shear and moment capacity:

$$\frac{V}{R_V} + \frac{M}{R_M} = 1 \tag{16}$$

where R_V is the shear capacity, calculated as the bonding strength multiplied by the total glued area, and R_M is the moment capacity, estimated using the analytical model proposed in [30]. It should be noted that the bonding strength values used in this study were estimated based on the size of the glued area compared to that in [30]. However, these values are approximated, and further investigation is required to obtain more precise values for accurately estimating the bonding resistance of large glued areas.

2.3.2.2 Numerical models

Two-dimensional numerical models of the truss specimens were developed using Abaqus CAE 6.25 (Simulia, USA). In these models, only the glulam beams were modelled as beam elements, as depicted in Figure 10. The assigned cross-section for the beams was 360x100 mm, consistent with the dimensions of the

tested specimens. Similarly to the analytical models (Figure 7), the connections between the beam elements were hinged for the mechanically connected trusses, while rigid for the adhesively bonded trusses, as shown in Figure 10.

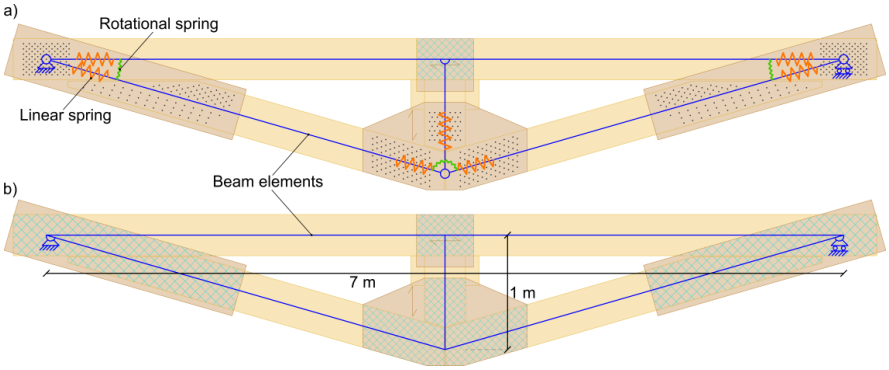

Figure 10: Illustration of numerical models: a) trusses with mechanical fasteners, b) glued trusses.

In addition, the stiffness of each fastener group for the trusses with mechanical connectors was considered by adding linear and rotational springs. The linear stiffness was calculated as the slip modulus per shear plane per fastener according to the equation for dowel type fastener in EC5 [16]:

$$K_{ser\_EC5} = {\rho_m}^{1.5} * \frac{d}{23} \tag{17}$$

where d is the fastener diameter and the factor ρ_m is the mean density of the timber elements, calculated as:

$$\rho_m = \sqrt{\rho_{Glulam} \cdot \rho_{Birch\ plywood}} \tag{18}$$

The stiffness of each fastener group was calculated by multiplying the stiffness of a single fastener (Equation 17) by the number of fasteners and shear planes.

Furthermore, the rotational stiffness of each fastener group per shear plane (K_θ) was based on the polar moment of inertia as [31]:

$$K_\theta = K_{ser\_EC5} * I_p \tag{19}$$

where K_{ser_EC5} is the slip modulus per shear plane per fastener (Equation 17) and I_p is the polar moment of inertia of the fastener group, calculated as:

$$I_p = \sum_{i=1}^{n} r_i^2 \tag{20}$$

where r_i is the distance from the centroid of each fastener to the geometrical centroid (centre of gravity) of the fastener group.

The material properties assigned to the glulam beams are shown in Table 1. The elastic and shear modulus values correspond to GL24h glulam in EN 14080:2013 [32], Poisson's ratios were taken from [33], and the density is the measured mean value from sample specimens (Section 2.3.1).

Table 1: Mechanical properties of glulam beams used in the numerical model. E_{ii} are the elastic modulus, υ_{ij} are the poisson's ratios, G_{ij} are the shear modulus and ρ is the density.

E_{11} [MPa]	E_{22} [MPa]	E_{33} [MPa]	υ_{12}	υ_{13}
11500	300	300	0.0097	0.0097
υ_{23}	G_{12} [MPa]	G_{13} [MPa]	G_{23} [MPa]	ρ [kg/m^3]
0.582	650	650	65	524.2

Furthermore, the non-linearity of both timber elements and steel dowels was not modelled since the designed failure mode was in the central plywood plate in tension with no yielding of the fasteners.

3 Results

3.1 Lateral load-carrying capacity

3.1.1 Experimental results

All specimens showed ductile behaviour and most reached the maximum load at 15 mm of slip with no significant load drop, as shown in Figure 11. As defined by ISO 6891-1983 (E) [22], the load-carrying capacity of a connection is the highest recorded load within 0 and 15 mm of slip.

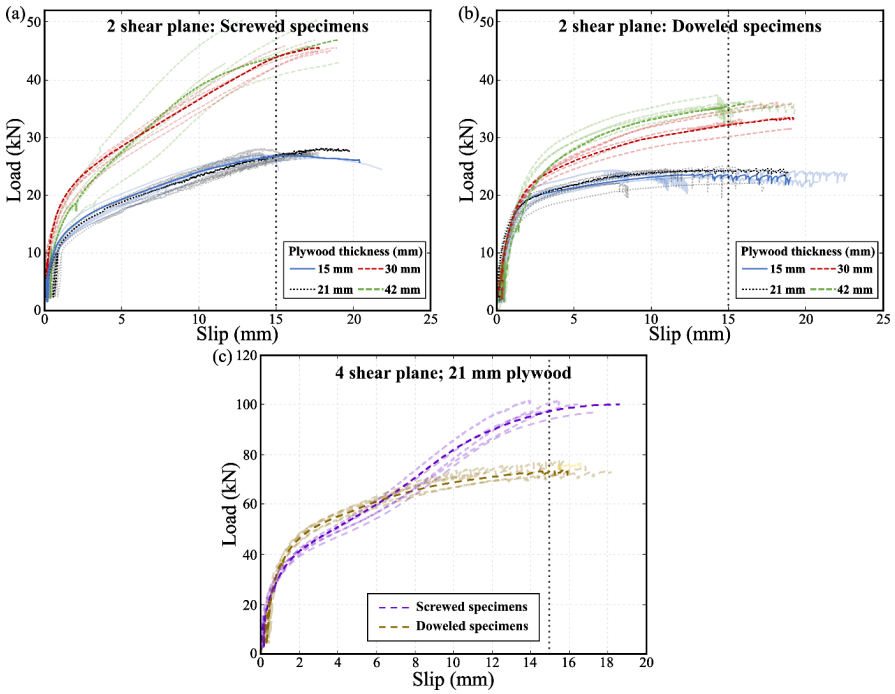

Figure 11: Load-slip curves for: a) specimens in double shear with screws, b) specimens in double shear with dowels, and c) all specimens with four shear planes.

Comparing specimens in double shear using screws to the ones using dowels reveals that, after the fastener yields, the ones with dowels tend to reach a plateau, at least when the thickness of the plywood is 21 mm or less. In contrast, the load continues to increase significantly for specimens with screws, showing

steeper gradients when the plywood is 30 mm thick or more. Furthermore, for specimens with thinner plywood plates, the resulting load-carrying capacity of the specimens with screws was higher than those with dowels, even though the screws started to yield at lower load levels compared to the dowels. These differences have been attributed to the rope effect, whereby an axial force arises in the fastener after significant bending. This axial force has a component parallel to the applied load, which helps carry the load, and a perpendicular component that increases friction between the timber members.

For specimens with four shear planes, after the yielding of the fasteners, the hardening of the specimens using screws is more significant as compared to those with dowels, thus resulting in a higher load-carrying capacity. Furthermore, as compared to the specimens in double shear, the hardening for specimens with four shear planes is more significant regardless of the type of fastener. This was associated with the failure mode in the inner shear planes, in which the fastener deforms and gets anchored, which makes it act as a stress ribbon due to the horizontal restrain for translations at the mid-support [34]. This allows part of the load to be transferred through tensile force in the fastener, thus increasing the overall load-carrying capacity.

3.1.2 Comparison between analytical predictions and experiments

3.1.2.1 Failure modes

Experiments showed generally good agreement with the analytically predicted failure modes. As shown in Figure 12, all specimens in double shear with 15 and 21 mm thick plywood plates showed failure *mode j* with the formation of one plastic hinge per shear plane, while specimens with 42 mm plywood showed failure *mode k* with the formation of two plastic hinges per shear plane. Despite the predicted failure mode for specimens with 30 mm plywood and screws was *mode k*, only some screws showed failure *mode k* while most showed *mode j*. In addition, approximately half of the specimens with 30 mm plywood and dowels exhibited failure *mode k*, although predicted failure was *mode j*.

Specimens with four shear planes exhibited failure *mode j* in the outer shear planes and failure *mode k* in the inner ones, in agreement with analytical estimations.

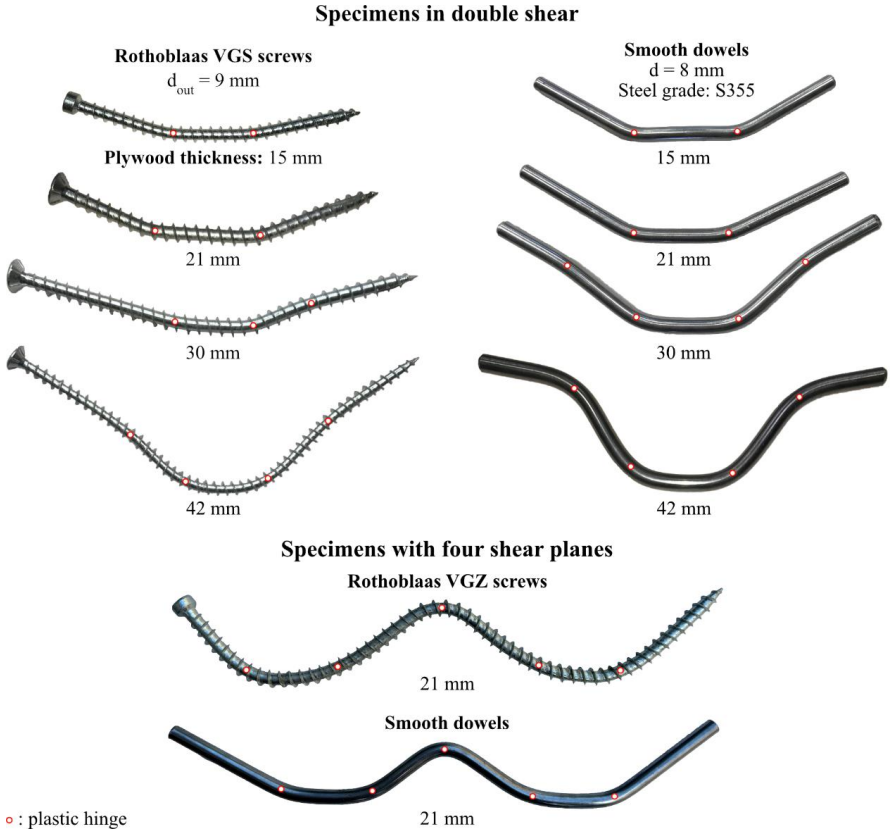

Figure 12: Experimental failure modes of mechanical fasteners for all specimens.

3.1.2.2 Load-carrying capacity

Figure 13 compares the analytical and mean experimental load-carrying capacity per fastener for specimens in double shear and the mean capacity of the inner shear planes in specimens with four shear planes. The experimental capacity of the inner shear planes in specimens with four shear planes was determined by subtracting the mean capacity of the outer shear planes from the total mean experimental capacity. The outer shear planes' capacity was assumed to match that of the specimens in double shear with the same plywood plate thickness (21 mm).

The analytical estimations generally underestimate the experimental load-carrying capacity of specimens in double shear, especially for the specimens with screws and thicker plywood plates. For specimens with four shear planes, the mean experimental capacity of the inner shear planes is significantly higher than

the analytical estimations. Furthermore, the experimental capacity of the inner shear planes is almost three times that of the specimens in double shear with the same plywood thickness (21 mm) when using screws, and approximately double when using smooth dowels. This discrepancy was associated with the failure mode in the inner shear planes, in which the fastener deforms and gets anchored, thus increasing the load-carrying capacity, as explained in Section 3.1.1.

Moreover, the pre-drilling appeared to slightly reduce the load-carrying capacity for the screwed specimens with 30 mm thick plywood, although EC5 [16] requires to pre-drill before the assembly.

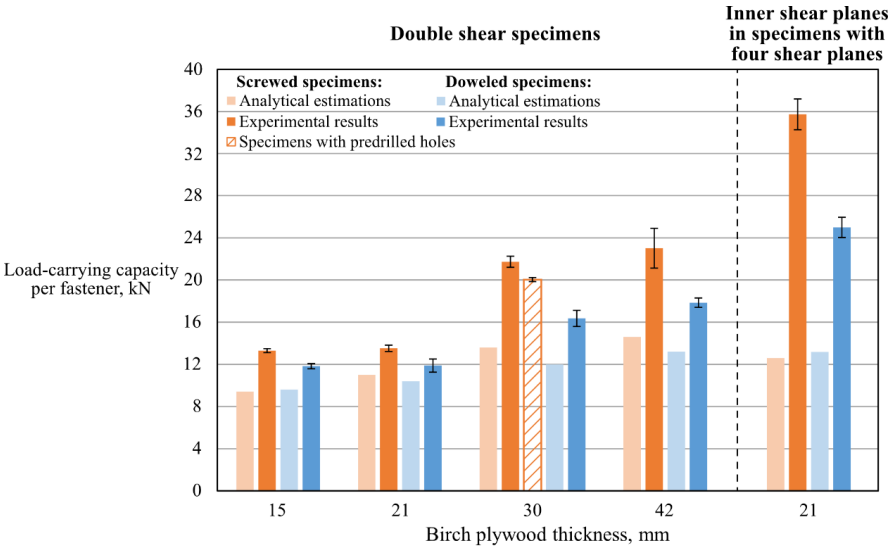

Figure 13: Analytical and mean experimental load-carrying capacity per fastener for specimens in double shear and inner shear planes for specimens with four shear planes. The error bars correspond to the standard deviation.

Table 2 shows further details regarding the analytical estimations and the experimental results of the load-carrying capacity per fastener for specimens in double shear. As presented in Section 2.2.2, the analytical estimations are the sum of the dowel effect and rope effect contributions. Furthermore, from the mean experimental capacity ($F_{experimental}$), the yielding capacity ($F_{yielding}$) was estimated as the load at which the yielding of the fasteners occurred, as a comparison to Johansen's theoretical contribution (dowel effect part). The post-yielding capacity ($F_{post\text{-}yielding}$) was estimated as the difference between the mean experimental and the yielding capacity. Further details about how they were calculated are presented in Paper I [23].

The obtained yielding capacity shows a fairly strong correlation with the dowel effect part from the analytical estimations. This is reasonable since the dowel-effect part is Johansen's theoretical contribution, which estimates the fastener yielding for failure *modes j* and *k*. Furthermore, it can be noted that the post-yielding capacity of all specimens generally increases as the plywood thickness increase and is significantly higher for specimens with screws. For smooth dowels, according to the analytical calculations in EC5 [16], after the yielding, the load-slip curve should reach a plateau, leading to no further load increase. However, according to the experimental results of this study, specimens with dowels showed a slight load increase after the fastener yielding, which is directly related to the plywood thickness. This might be due to friction between the timber and the fastener that can activate some tensile force in the dowel, as observed in [35].

Table 2: Analytical and experimental load-carrying capacity per fastener comparison for specimens in double shear. The values within brackets are the coefficients of variation.

Plywood thickness, mm	Specimens with screws					
	Analytical estimations			Mean experimental capacity		
	Dowel effect, kN	Rope effect, kN	Dowel + rope, kN	$F_{yielding}$, kN	$F_{post\text{-}yielding}$, kN	$F_{experimental}$, kN
15	7.84	1.67	9.51	8.13	5.17	13.4 (1.5 %)
21	8.83	2.26	11.1	8.30	5.23	13.6 (2.2 %)
30	10.3	3.11	13.4	12.7	9.05	21.8 (2.4 %)
42	10.3	4.21	14.5	15.0	8.03	23.0 (8.2 %)
	Specimens with dowels					
15	9.61	-	-	10.3	1.49	11.8 (2.1 %)
21	10.3	-	-	9.93	1.95	11.9 (5.3 %)
30	12.0	-	-	13.3	3.09	16.4 (4.6 %)
42	13.2	-	-	14.8	3.09	17.9 (2.5 %)

Furthermore, for specimens with screws, the post-yielding capacity is a significant contribution to the experimental capacity, being approximately 40 % of the experimental capacity regardless of the plywood thickness. According to the analytical calculations following EC5 [16], the contribution from the rope effect on the overall capacity for screws varies from 17 % for specimens with the thinnest plywood plates up to 29 % for those with the thickest plates. Moreover,

the analytical estimations of the rope effect are significantly smaller than the corresponding post-yielding capacity, meaning that EC5 significantly underestimates its contribution.

3.1.2.3 Plastic hinge location

The mean experimental location of the plastic hinges was estimated and compared to the analytical estimations according to Johansen's theoretical model for the specimens in double shear. According to this theory, the portion of the cross-section between the plastic hinge and the plywood-timber interface is bearing the load, as depicted in Figure 6. After testing, the specimens were opened and this portion was estimated and referred to as b. A semi-analytical capacity ($F_{v,semi\text{-}analytical}$) was calculated based on the values of b according to the equation below:

$$F_{v,semi-analytical} = n \cdot f_{h,C24} \cdot b_{experimental} \cdot d \quad (21)$$

where n is the number of shear planes; $f_{h,C24}$ is the embedment strength of the structural timber; $b_{experimental}$ is the value of b estimated from the experiments; and d is the diameter of the fastener.

The mean experimental and analytical values of b, together with the semi-analytical and mean experimental capacity per fastener are shown in Table 3.

Table 3: Comparison of analytical and experimental location of plastic hinges, semi-analytical and mean experimental capacity per fastener for specimens in double shear. The values within brackets are the coefficients of variation.

Plywood thickness, mm	Specimens with screws			
	$b_{analytical}$, mm	$b_{experimental}$, mm	$F_{v,semi\text{-}analytical}$, kN	$F_{experimental}$, kN
15	14.5	21.6 (8.8 %)	11.6	13.4
21	16.4	23.4 (16.5 %)	12.6	13.6
30	19.4	30.1 (11.6 %)	16.2	21.8
42	19.4	28.6 (16.7 %)	15.4	23.0
	Specimens with dowels			
15	15.3	15.3 (7.0 %)	9.58	11.8
21	16.6	20.5 (4.0 %)	12.8	11.9
30	19.2	24.7 (16.0 %)	15.5	16.4
42	21.1	22.7 (4.6 %)	14.2	17.9

Specimens with dowels generally showed satisfactory agreement between experimental and analytical estimations in terms of plastic hinge location, despite exhibiting different values of $b_{experimental}$ and $b_{analytical}$ for 21 mm and 30 mm thick plywood. Furthermore, for specimens with dowels, the semi-analytical capacity is generally consistent with the mean experimental results. The small discrepancies may be due to variations in the local embedment strengths of the timber compared to the mean value. In contrast, for specimens with screws, $b_{experimental}$ was significantly larger than the analytical predictions. This observation can be attributed to the tensile force that develops in the screw, which is not considered in Johansen's theoretical model. This force could shift the location of the plastic hinges and increase *b*, which is the portion of the cross-section which is bearing the load, thus increasing the load-carrying capacity [15]. In addition, for specimens with screws, the experimental capacity is higher than the semi-analytical capacity. This is because, due to the rope effect, the screws are also activated in tension; however the tensile force in the screws is not considered in the calculation of the semi-analytical capacity.

3.2 Full-scale glulam trusses with birch plywood gusset plates

3.2.1 Experimental results

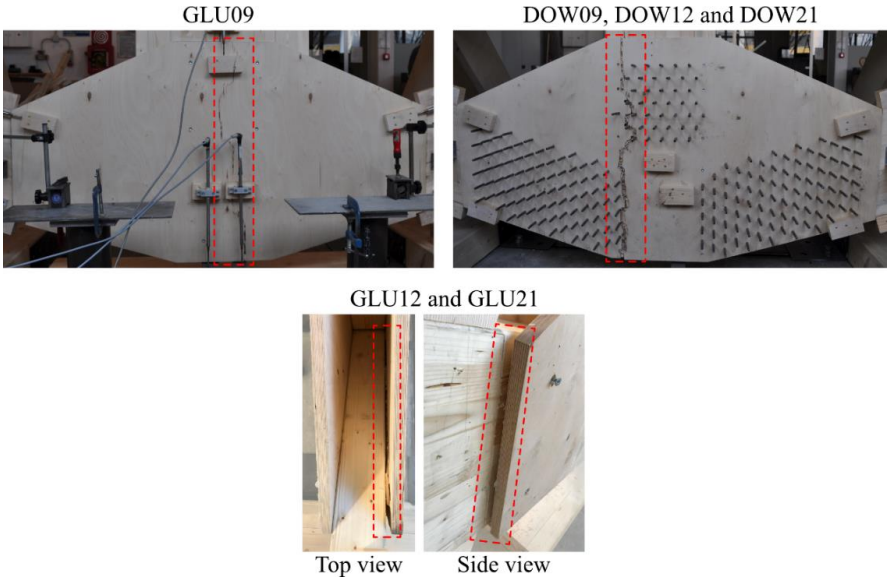

Figure 14: Typical failure modes.

The glued specimen with the thinner central plywood plates, i.e. GLU09, and all doweled trusses failed in the central plywood plates, as shown in Figure 14. Plywood failure occurred as a vertical crack along the entire height of the plywood plate, following the fastener line in specimens with mechanical connectors and the symmetry line in specimen GLU09. The glued specimens with thicker central plywood plates, i.e. GLU12 and GLU21, failed in the glue line between the inclined glulam members and the central plywood plate.

The maximum recorded load (F_{max}) and displacement (u_{Fmax}), and the global experimental stiffness (K_{exp}), calculated as the linear slope of the load-displacement curve between 10 % and 40 % of F_{max} are presented in Table 4. The displacement data used for estimating the experimental stiffness is the absolute displacement measured on the midpoint of the central plywood plate, taken from the LVDT labelled as "Middle Vertical" [26].

Table 4: Maximum experimental loads and displacements, and global experimental stiffness.

ID	F_{max} [kN]	u_{Fmax} [mm]	K_{exp} [kN/mm]
GLU09	146.7	13.9	12.1*
GLU12	202.0	21.7	11.1
GLU21	289.4	30.6	10.3
DOW09	111.3	18.0	6.34
DOW12	183.7	30.6	6.38
DOW21	264.4	46.7	6.36

*mean displacement from the LVDTs "East Vertical" and "West Vertical" [26].

Glued specimens showed higher maximum load (F_{max}) than those using mechanical connectors because the plywood plates required predrilling for the insertion of the fasteners that reduce the net cross-section, thus weakening the plate. In addition, glued specimens possess almost double global stiffness than those mechanically connected. Moreover, the stiffness of both glued and doweled trusses seems to be independent on the thickness of the central plywood plate, as suggested by EC5 [16].

Figure 15 shows the load-jack displacement curves for all specimens. As expected, F_{max} was proportional to the thickness of the central plywood plate for specimens that exhibited plywood failure. Furthermore, these specimens

showed linear elastic behaviour until brittle failure occurred. The glued trusses that failed in the glue line (GLU12 and GLU21) showed very small signs of ductility for unknown reasons. These trusses showed an unexpected discrepancy in the ultimate load, although the size of the glued area was the same. The reason for such discrepancy is discussed in section 3.2.3.

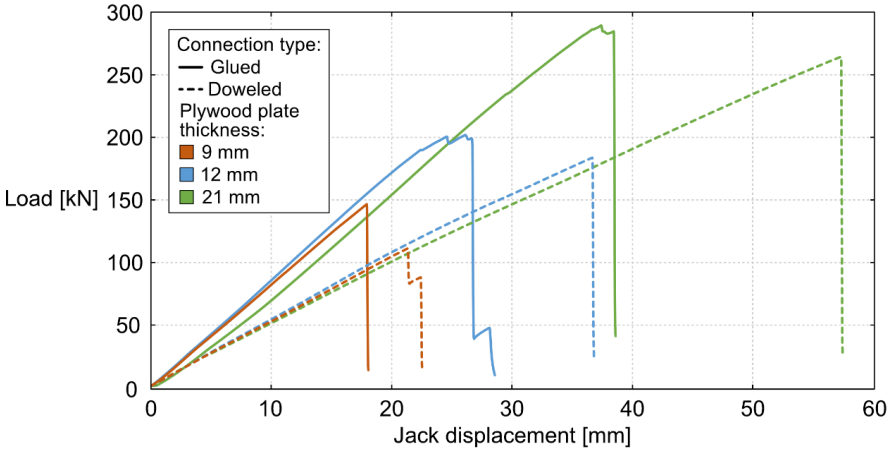

Figure 15: Load-jack displacement curves for all specimens.

3.2.2 Prediction models

3.2.2.1 Analytical models

The results of analytically calculated maximum loads and predicted failure modes are compared to the maximum experimental load (F_{max}) and shown in Table 5. In addition, the ratio between the analytically predicted failure load and the maximum experimental load (F_{max}) is shown in Table 5. Furthermore, failure of the glulam beams and compressive failure of the birch plywood plates at the connection to the vertical post were also analysed; however, the results are not included, as they exhibited higher estimated failure loads.

The expected failure mode for glued trusses is the tensile failure of the central plywood plate for specimens with thinner plywood (GLU09 and GLU12). For specimen GLU21, the expected failure mode is along the glue line between the central plywood plate and the inclined glulam beam. However, as previously mentioned, the bonding strength values used in the analytical estimations are approximated, and further investigation is required to obtain more precise values for accurately estimating the bonding resistance of large glued areas. The significant overestimation of the experimental bonding resistance of specimen GLU12, as discussed in detail in Section 3.2.3, is attributed to the low value of

wood failure percentage (WFP). Furthermore, for trusses with mechanical connectors, the expected failure mode is the tensile failure of the central plywood plate, regardless of the plywood thickness.

Table 5: Analytically calculated failure loads and modes, maximum experimental load, and the ratio between analytical and experimental load. The values in bold are the expected failure modes.

ID	$F_{analytical}$ [kN]		F_{max} [kN]	Ratio
	Tensile failure plywood	Glue line failure		
GLU09	**162.6**	264.0	146.7	1.11
GLU12	**216.8**	264.0	202.0	1.07
GLU21	379.4	**264.0**	289.4	0.912
DOW09	**137.5**	-	111.3	1.24
DOW12	**183.3**	-	183.7	0.998
DOW21	**320.9**	-	264.4	1.21

The analytical estimations for specimens that failed in the plywood plate, i.e. all trusses with mechanical connectors and GLU09, showed good agreement with the experimental results. The analytical estimations are slightly overestimating the experimental capacity, except for specimen DOW12. This was expected and is attributed to the size effect, as the input strength values of plywood adopted in the analytical estimations were obtained from small-scale tests [4-5]. Furthermore, it should be noted that only one replicate was tested for each configuration, which may account for the variation observed in the ratio values.

3.2.2.2 Numerical models

The experimental global stiffness (K_{exp}) and the numerical global stiffness (K_{num}) are presented in Table 6. The numerical stiffness was defined as the ratio between the applied load and the displacement at the corresponding point used for the estimation of the experimental stiffness.

As shown in Table 6, the two-dimensional numerical models can satisfactorily predict the experimental stiffness. The results of the numerical stiffness for the trusses with mechanical connectors are significantly dependent on the input values of the linear and rotational springs' stiffness, which were both estimated according to Equation 17 [16]. However, it should be noted that

the thickness of the central plywood plate was intentionally under-designed, thus its deformability is not negligible and should therefore be considered in the numerical model [36]. This is particularly valid for specimens with mechanical connectors, as the lower region of the central plywood plate is free to deform due to the absence of fasteners (Figure 9). This is not happening for glued trusses since the contact area between the inclined glulam members and the central plywood plate was entirely glued.

Table 6: Experimental and numerical global stiffness.

ID	K_{exp} [kN/mm]	K_{num} [kN/mm]
GLU09	12.1*	9.85
GLU12	11.1	
GLU21	10.3	
DOW09	6.34	7.67
DOW12	6.38	
DOW21	6.36	

*mean displacement from the LVDTs "East Vertical" and "West Vertical" [26].

3.2.3 Glue line failure analysis

Glued specimens that showed glue line failure (i.e. GLU12 and GLU21) were opened to analyse the failure area in detail. The area where it was possible to see wood or wood fibres failure, was estimated and labelled as "actual glued area", as shown in Figure 16. A significant portion of the glued area, mainly close to the edges, did not show wood or wood fibres failure, especially for specimen GLU12 on side (b) and GLU21 on side (a). Except for specimen GLU21 on side (b), all the others showed mostly birch plywood failure in the first veneer with some glulam failure. This was expected, as in [37], a strong correlation between the bonding strength and the shear strength of the weaker wood adherent was found. In this case, the weaker adherent is birch plywood, as its face grain has an angle of 74° with the grain direction of the inclined glulam beam and is subjected to rolling shear due to the tensile force in the glulam.

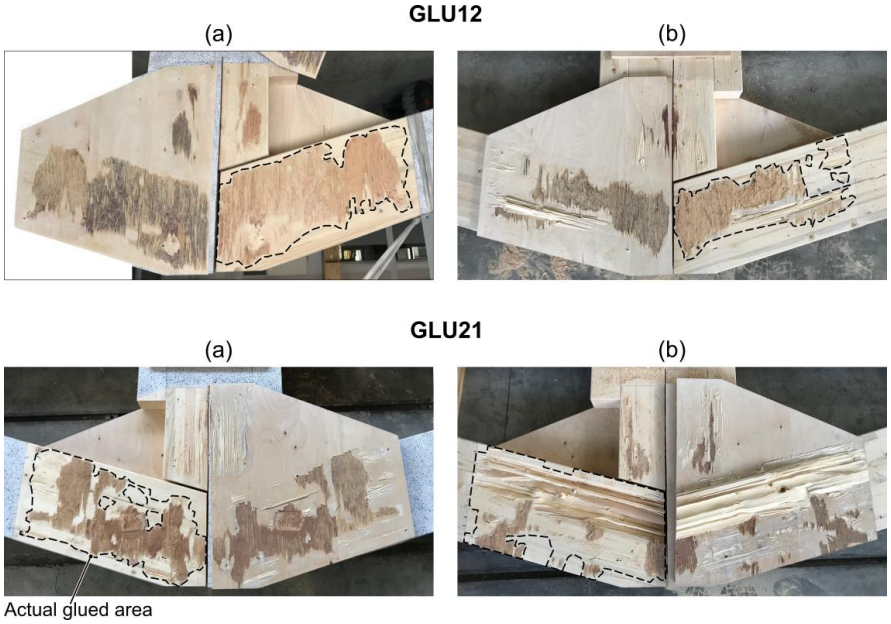

Figure 16: Glue line failures with the estimated portions of the "actual glued area" for specimens GLU12 and GLU21.

Table 7 presents the values of the estimated actual glued area, nominal glued area and the wood failure percentage (WFP). The nominal glued area is the contact area between the plywood plate and the inclined glulam beam, while the WFP values were calculated as the ratios between actual and nominal glued areas.

Table 7: Nominal and actual glued areas, and WFP for specimens that showed glue line failure.

ID	Side	Nominal glued area [cm²]	Actual glued area [cm²]	WFP [%]
GLU12	a	2648.7	1435.1	54.2
	b		2009.7	75.9
GLU21	a		2353.9	88.9
	b		1948.8	73.6

The lowest WFP value for specimen GLU12 was only about 54 %, while for GLU21 was 73 %. This difference can explain the discrepancy between these specimens in the maximum recorded load (F_{max}) in Table 4. The lowest WFP

value for specimen GLU21 was approximately 36 % larger than that of GLU12, while it possessed about 43 % higher F_{max} than GLU12.

Furthermore, the values of WFP are rather low, but the reasons for such low values are not straightforward to identify. For example, the amount of applied adhesive may have been insufficient, or the truss could have been moved before the complete curing of the glue, or the applied pressure during the curing process may not have been evenly distributed. In this case, the pressure was applied with clamps but due to the size of the glued area, it was not possible to guarantee an even pressure on the entire surface. Furthermore, this also depends on the out-of-plane stiffness of the plywood plate; the thicker the plate, the more evenly the pressure will be distributed. In addition, gluing connections such as truss nodes is more challenging due to their relatively large size and the varying shapes of the plywood. Therefore, screw-gluing is suggested as an alternative gluing method since it can guarantee a more evenly distributed pressure regardless of the size and shape of the connections.

4 Conclusions and future work

4.1 Conclusions

This thesis focused on investigating the performance of birch plywood gusset plates in timber connections, investigating both mechanical and adhesively bonded connections. The experimental and analytical studies aimed to evaluate load-carrying capacity, stiffness, and failure modes in both small-scale and full-scale structural applications.

The findings from the first paper indicate that Eurocode 5 (EC5) significantly underestimates the shear capacity of timber-to-birch plywood connections using screws due to a conservative estimation of the rope effect. The discrepancy becomes more pronounced as the number of shear planes increases, highlighting the need for a more accurate design model. Experimental results showed that connections with screws exhibited higher post-yielding capacity than those with dowels, primarily due to the activation of tensile force in the screws. Additionally, the plastic hinge locations in specimens with screws were shifted compared to the predictions according to Johansen's theoretical model, indicating the influence of the tensile force, which is not considered in the model.

The full-scale glulam truss tests demonstrated that glued trusses exhibited higher strength and significantly higher stiffness compared to mechanically connected trusses. The stiffness of glued trusses was almost double that of doweled trusses, and the failure occurred in the plywood plates for all mechanically connected trusses, as well as in the glued truss with the thinnest plywood plates (9 mm). However, in the glued trusses with thicker plywood plates (12 and 21 mm), failure occurred along the glue line between the plywood plate and the glulam beam. Despite slightly overestimating the experimental capacity for most specimens, analytical estimations generally provided good agreement with experimental results for specimens that failed in the central plywood plate. This overestimation was expected and attributed to the size effect, as the input strength values from the literature were obtained from small-scale experiments on birch plywood.

Furthermore, the analysis of glue line failure revealed relatively low values of wood failure percentage (WFP), indicating that clamping may not be the most effective method for large glued areas due to uneven pressure distribution.

Two-dimensional numerical simulations provided satisfactory predictions of the global stiffness. However, since the thickness of the central plywood plate was intentionally under-designed, its influence on the global stiffness is not really negligible, especially for specimens with mechanical connectors.

Overall, the results highlight the potential of birch plywood as an effective gusset plate for connections in timber structures. However, optimizing bonding techniques and analytical models is necessary to enhance reliability in full-scale structures.

4.2 Future work

To further develop the understanding and application of birch plywood gusset plates, the following future research is suggested:

- Improving EC5's lateral load-carrying capacity analytical model by refining the rope effect contribution;
- Size effect investigations on birch plywood mechanical properties, such as tension, shear and bending, and bonding strength, respectively;
- Perform more advanced 3D analysis for the truss specimens, e.g. by means of solid elements and non-linear analysis;
- Long-term investigations, such as creep deformation, on the behaviour of connections with birch plywood plates.

By addressing these aspects, future research can further enhance the safety, reliability, and efficiency of birch plywood gusset plates in timber connections.

References

[1] H.R. Milner, A.C. Woodard, (2016). Sustainability of engineered wood products, in: Sustain. Constr. Mater., Elsevier: pp. 159–180.

[2] T. Sellers, (1985). Plywood and adhesive technology, Marcel Dekker Inc, New York, ISBN 0824774078.

[3] U.S. Govt., Print. Off (1944), Design of wood aircraft structures. https://doi.org/10.5479/sil.1018746.39088017549809.

[4] T. Wang, Y. Wang, R. Crocetti, M. Wålinder, In-plane mechanical properties of birch plywood, Construction and Building Materials, Volume 340, 2022, 127852, ISSN 0950-0618, https://doi.org/10.1016/j.conbuildmat.2022.127852.

[5] T. Wang, Y. Wang, R. Crocetti, M. Wålinder, Influence of face grain angle, size, and moisture content on the edgewise bending strength and stiffness of birch plywood, Materials & Design, Volume 223, 2022, 111227, ISSN 0264-1275, https://doi.org/10.1016/j.matdes.2022.111227.

[6] Y. Wang, T. Wang, R. Crocetti, M. Schweigler, M. Wålinder, Embedment behavior of dowel-type fasteners in birch plywood: Influence of load-to-face grain angle, test set-up, fastener diameter, and acetylation, Construction and Building Materials, Volume 384, 2023, 131440, ISSN 0950-0618, https://doi.org/10.1016/j.conbuildmat.2023.131440.

[7] Y. Wang, T. Wang, M. Debertolis, R. Crocetti, M. Wålinder, "Design of birch plywood as gusset plates in timber-timber uniaxial tension connections: Influence of fastener pattern, face grain orientation, and discussions based on the Whitmore effective width theory", Journal of Building Engineering, Volume 86, 2024, 108796, ISSN 2352-7102, https://doi.org/10.1016/j.jobe.2024.108796.

[8] T. Wang, Y. Wang, M. Debertolis, R. Crocetti, M. Wålinder, L. Blomqvist, Spreading angle analysis on the tensile capacities of birch plywood plates in adhesively bonded timber connections, Engineering Structures, Volume 315, 2024, 118428, ISSN 0141-0296, https://doi.org/10.1016/j.engstruct.2024.118428.

[9] Y. Wang, Mechanical connections using birch plywood as gusset plates in timber structures (PhD dissertation, KTH Royal Institute of Technology), 2024. Retrieved from: https://urn.kb.se/resolve?urn=urn:nbn:se:kth:diva-345772.

[10] Y. Wang, T. Wang, M. Debertolis, R. Crocetti, M. Wålinder, L. Blomqvist, Glulam frame corner joints built of birch plywood and mechanical fasteners: An experimental,

analytical, and numerical study, Engineering Structures, Volume 310, 2024, 118112, ISSN 0141-0296, https://doi.org/10.1016/j.engstruct.2024.118112.

[11] Y. Wang, T. Wang, J. Ringaby, R. Crocetti, M. Debertolis, M. Wålinder, Testing and analysis of screw-connected moment joints consisting of glued-laminated timbers and birch plywood plates, Engineering Structures, Volume 290, 2023, 116356, ISSN 0141-0296, https://doi.org/10.1016/j.engstruct.2023.116356.

[12] C. Sandhaas, H. J. Blaß, (2017). Timber Engineering - Principles for Design. Karlsruhe: KIT Scientific Publishing. DOI: https://doi.org/10.5445/KSP/1000069616.

[13] M. L. Batchelar, K. A. McIntosh, (1998). Structural joints in glulam. Proc., 5th World Conf. on Timber Engineering, Natterer, J. and Sandoz, J.-L., eds., Vol. 1, Montreux, Switzerland, 289–296.

[14] Z. Duan, Q. Huang, Q. Zhang, Life cycle assessment of mass timber construction: A review, Build. Environ. 221 (2022) 109320. https://doi.org/10.1016/j.buildenv.2022.109320.

[15] R. Crocetti, K. Lappalainen, M. Backman, M. Wålinder, J. Norén, Multiple shear plane connections with timber based gusset plates, in: World Conf. Timber Eng. 2021, WCTE 2021, 9th August 2021 through 12th August 2021, Santiago, Chile.

[16] EN1995-1-1: Eurocode 5: Design of timber structures - Part 1-1: General - Common rules and rules for buildings. The European Union Per Regulation 305/2011, Directive 98/34/EC, Directive 2004/18/EC, 2004.

[17] T. Wang, Y. Wang, R. Crocetti, M. Wålinder, Multiple Shear Plane Timber Connections with Birch Plywood and Dowel-Type Fasteners, in: Laureckienė Ginta (ed) Proceedings of the 17th Annual Meeting of the Northern European Network for Wood Science and Engineering (WSE2021). Kaunas University of Technology, Kaunas: 131–133.

[18] M. Schweigler, M. Vedovelli, R. Lemaître, J.F. Bocquet, C. Sandhaas, T. K. Bader, Beam-on-Foundation Modeling as an Alternative Design Method for Timber Joints with Dowel-Type Fasteners –Part 3: Second Order Theory Effects for Considering the Rope Effect, 54th International Network on Timber Engineering Research (INTER) meeting proceedings, 2021, ISSN 2199-9740.

[19] T. Gečys, T. K. Bader, A. Olsson, S. Kajėnas, Influence of the rope effect on the slip curve of laterally loaded, nailed and screwed timber-to-timber connections, Construction and Building Materials, Volume 228, 2019, 116702, ISSN 0950-0618, https://doi.org/10.1016/j.conbuildmat.2019.116702.

[20] Handbook of Koskisen Plywood. Retrieved from: https://koskisen.fi/en/downloads/ [accessed on 07/03/2025].

[21] Rothoblaas Srl, TIMBER SCREWS AND DECK FASTENING Catalogue, Cortaccia, 2023, https://issuu.com/rothoblaas/docs/timber-screws-and-deck-fastening-2023-en?mode=embed.

[22] ISO 6891-1983 (E): Timber structures – Joint made with mechanical fasteners – General principles for the determination of strength and deformation characteristics, International Organisation for Standardizations, 1983.

[23] M. Debertolis, Y. Wang, T. Wang, R. Crocetti, M. Wålinder, Rope effect in mechanical panel-timber connections: A comparison between screws and dowels, Engineering Structures, Volume 332, 2025, 120036, ISSN 0141-0296, https://doi.org/10.1016/j.engstruct.2025.120036.

[24] EN 322:1993, Wood-based panels – Determination of moisture content, European Committee for Standardization (CEN), 1993.

[25] Design of timber structures Volume 1, Structural aspects of timber constructions, 2nd edition, Swedish Wood, 2016, ISBN 978-91-980304-8-8.

[26] M. Debertolis, Y. Wang, T. Wang, R. Crocetti, M. Wålinder, P. Rigo, A. Polastri, "Analytical, experimental and numerical investigation on full-scale glulam trusses joined through birch plywood plates". *Submitted manuscript*.

[27] EN 13183-1:2002, Moisture content of a piece of sawn timber – Part 1: Determination by oven dry method, European Committee for Standardization, 2002.

[28] T. Wang, In-plane mechanical properties of birch plywood and its performance in adhesively bonded connections (PhD dissertation, KTH Royal Institute of Technology), 2024. Retrieved from: https://urn.kb.se/resolve?urn=urn:nbn:se:kth:diva-344306.

[29] D. King, A. Van Houtte, NZ Wood Design Guides NZ Wood Design Guide 12.5: Portal Knee Connections 2, 2020, http://nzwooddesignguides.

[30] T. Wang, Y. Wang, J. Ringaby, R. Crocetti, M. Wålinder, L. Blomqvist, Glulam beams adhesively bonded by birch plywood plates in moment-resisting beam-to-beam connections, Engineering Structures, Volume 302, 2024, 117471, ISSN 0141-0296, https://doi.org/10.1016/j.engstruct.2024.117471.

[31] X.T. Wang, E.C. Zhu, S. Niu, H.J. Wang, Analysis and test of stiffness of bolted connections in timber structures, Construction and Building Materials, Volume 303, 2021, 124495, ISSN 0950-0618, https://doi.org/10.1016/j.conbuildmat.2021.124495.

[32] EN 14080:2013, Timber structures – Glued laminated timber and glued solid timber – Requirements, European Committee for Standardization, 2013.

[33] M. Dorn, Investigations on the Serviceability Limit State of Dowel-Type Timber Connections, Vienna, Austria, 2012, PhD dissertation, https://repositum.tuwien.at/handle/20.500.12708/13320.

[34] S. Rossi, R. Crocetti, D. Honfi, E. Frühwald Hansson, Load-bearing capacity of ductile multiple shear steel-to-timber connections, in: World Conf. Timber Eng. 2016, WCTE 2016, 22nd August 2021 through 25th August 2021, Vienna, Austria.

[35] M. Schweigler, M. Vedovelli, R. Lemaître, J.F. Bocquet, C. Sandhaas, T. K. Bader, Beam-on-Foundation Modeling as an Alternative Design Method for Timber Joints with Dowel-Type Fasteners –Part 3: Second Order Theory Effects for Considering the Rope Effect, 54th International Network on Timber Engineering Research (INTER) meeting proceedings, 2021, ISSN 2199-9740.

[36] Y. Wang, T. Wang, P. Persson, P. Hedlund, R. Crocetti, M. Wålinder, Birch plywood as gusset plates in glulam frame via mechanical connectors: A combined experimental and numerical study, Journal of Building Engineering, Volume 65, 2023, 105744, ISSN 2352-7102, https://doi.org/10.1016/j.jobe.2022.105744.

[37] T. Wang, Y. Wang, M. Debertolis, R. Crocetti, M. Wålinder, L. Blomqvist, Bonding strength between spruce glulam and birch plywood at different load-to-plywood face grain angles. Eur. J. Wood Prod. 82, 1407–1419 (2024). https://doi.org/10.1007/s00107-024-02097-9.